Revision # 2

Low intra-crystalline closure temperatures of Cr-bearing spinels from the mantle xenoliths of the Middle Atlas Neogene-Quaternary Volcanic Field (Morocco): A mineralogical evidence of a cooler mantle beneath the West African Craton

Davide Lenaz[1*], Nasrrddine Youbi[2,3], Angelo De Min[1], Moulay Ahmed Boumehdi[2], and Mohamed Ben Abbou[4]

[1]Department of Mathematics and Geosciences, Università degli Studi di Trieste, Via Weiss 8, 34127 Trieste, Italy, lenaz@units.it; demin@univ.trieste.it

[2]Geology Department, Faculty of Sciences-Semlalia, Cadi Ayyad University, Prince Moulay Abdellah Boulevard, P.O. Box 2390, 40 000 Marrakech, Morocco, e-mail: youbi@uca.ma

[3]Centro de Geologia da Universidade de Lisboa (CeGUL), Faculdade de Ciências (FCUL), Departamento de Geologia (GeoFCUL), Campo Grande C6, 1749-016 Lisboa, Portugal

[4]Geology Department, Faculty of Sciences Dhar Al Mahraz, Sidi Mohammed Ben Abdellah University, P.O. Box 1796, Fès-Atlas, 30003 Fès, Morocco

*Corresponding author: Davide Lenaz, lenaz@units.it

ABSTRACT

The crystal chemistry of nine Cr-spinels from lherzolite and harzburgite xenoliths from the Middle Atlas Neogene-Quaternary Volcanic Field of Morocco have been studied by means of X-ray single crystal diffraction and electron microprobe analyses. Cell edges are usually within the range 8.13-8.14 Å, but there are three samples with longer *a* value, so that the whole analyzed series is within the range 8.1334 (4) – 8.2021 (2) Å, while the oxygen positional parameter values are very similar ranging between 0.2626 (1) and 0.2629 (2) for all of them. The cation distribution shows that the crystal structure is ordered with almost all divalent cations in the tetrahedral site and trivalent cations in the octahedral site. The determined intracrystalline temperatures are in the range 550-

750°C, that are the lowest values ever found for Cr-spinels from mantle xenoliths as these are usually higher than 730°C. If we consider the behavior of some geotherms from literature, the determined temperatures are confined in a depth range of about 20-40 Km. Lithospheric models for the studied area indicate that the lower crust reaches its deepest value in a range between 30 and 40 Km. Consequently, we can assume that the studied xenoliths were emplaced at a "shallow" depth of about 20-30 Km, just beneath the lower crust, where they were disrupted and brought to the surface from the ascending alkaline lavas. This assumption is consistent with the concomitant presence of some crustal xenoliths. It is important to notice that even in the case of a mantle xenoliths where all the silicates could be heavily altered, the presence of one single crystal of Cr-spinel and the study of its oxygen coordinates (*u*), inversion parameters (*i*), Cr content, and calculated closure temperatures can be used to validate the thermal history of the mantle xenoliths. The combined approach of structural data, intra- and inter-crystalline temperatures and the literature geophysical data seems to be an interesting tool to assess the pre-exhumation history of the mantle xenoliths.

KEYWORDS: Cr-spinels, mantle xenoliths, crystal chemistry, intracrystalline temperature, Morocco.

Introduction

The structures and site occupancies of natural and synthetic Cr-bearing spinels have been extensively studied using single-crystal X-ray diffraction techniques and various spectroscopies in the past 25 years (Della Giusta et al. 1986; Princivalle et al. 1989; Carbonin et al. 1996, 1999; Della Giusta et al. 1996; Lenaz and Princivalle 1996, 2005; Lenaz et al. 2002, 2004a, 2004b, 2006, 2010, 2013; Carraro 2003; Bosi et al. 2004; Uchida et al. 2005; Nédli et al. 2008; Derbyshire et al. 2013; Lenaz and Lughi 2013; Lenaz and Skogby 2013) because of their importance as petrogenetic indicators, geobarometers, geothermometers and ore minerals for Cr and platinum group elements extraction.

The unit cell of the spinel structure can be described as a slightly distorted cubic close-packed (ccp) array of 32 oxygen atoms with 8 cations at tetrahedrally coordinated T sites, and 16 cations at octahedrally coordinated M sites (Hill et al. 1979). The T and M sites lie on special positions with -43m and -3m symmetry, respectively. The only variable geometrical parameters are the unit-cell edge (a) and oxygen coordinate (u,u,u), which is related to the oxygen packing distortion. The ideal ccp structure shows $u = 0.25$, but it is observed that $u > 0.25$ for all the Cr-bearing spinels. The observed distortion is a consequence of similar M-O and T-O bond distances ($u = 0.2625$ when distances are equal; Hill et al. 1979).

By the middle of the 80s, single crystal diffraction studies on Cr bearing spinels from mantle xenoliths started (Della Giusta et al. 1986; Princivalle et al. 1989) continuing till today (Carraro 2003; Uchida et al. 2005; Nédli et al. 2008). Princivalle et al. (1989) observed that u displays a constant value within the spinels from individual geological settings, even if there is a variation in bulk chemistry, whereas spinels with similar bulk chemistry but belonging to different geological environments exhibit a wide range of u values.

Mantle xenoliths enclosed in the Plio-Quaternary alkaline basalts from the Middle Atlas, Morocco, are characterized by a wide range of lithological and chemical heterogeneity, consistent with metasomatism of their lithospheric mantle source (Raffone et al 2009). They consist of porphyroclastic to protogranular spinel-lherzolites associated with websterites exhibiting major and trace element signatures, along with a depleted mantle isotopic affinity, testifying ancient melt extraction processes, possibly during Neo- to Paleoproterozoic times. This scenario is similar to that inferred for other Cenozoic Central-Northern African volcanic centers, such as Hoggar (Algeria; Beccaluva et al. 2007) and Gharyan (Libya; Beccaluva et al. 2008; Raffone et al. 2009). Previous studies on the mineral phases present in these xenoliths include REE analyses of clinopyroxenes. Isotope and trace element variability found in these xenoliths supports a multistage metasomatic process in which clinopyroxene and amphibole are recent secondary additions to the lithospheric mantle (Malarkey et al. 2011). The Pb isotope evolution of the clinopyroxenes suggests that there was a metasomatic enrichment younger than 200 Ma, which discounts the volcanic activity due to the opening of the Atlantic and the onset of the collision of the African and Eurasian plates as processes generating the lithophile element and isotope composition of this continental mantle root. Instead, the enrichment is thought to be associated with the Quaternary intra-plate volcanism in the Middle Atlas, and probably due to a carbonatitic metasomatism (Wittig et al. 2010). To our knowledge no previous crystallographic studies exist on the mineral phases of these xenoliths. The aim of this study is to analyze the structure of the Cr-bearing spinel, to calculate the cation distribution and, consequently, infer some information about the intracrystalline closure temperature of the spinels themselves. Successively these information will be compared with those of other Cr-spinels from mantle xenoliths worldwide.

Geological setting and sampling.

The Cenozoic volcanism of the Atlas system is exclusively of intraplate alkaline type (alkali basalts, basanites, nephelinites, and associated intermediate and evolved lavas), while in the Rif it evolved through time from calc-alkaline to shoshonitic and finally alkaline magmas (Hernandez and Bellon 1985; Hernandez et al. 1987; Berrahma and Delaloye 1989; Berrahma et al. 1993; El Bakkali et al. 1998, El Azzouzi et al. 1999, 2010; Maury et al. 2000, Duggen et al. 2005, 2009). It is located within a SW-NE trending volcanic strip (Fig. 1, inset), underlain by thinned lithosphere (Frizon de Lamotte et al. 2004; Teixell et al. 2005; Zeyen et al. 2005; Missenard et al. 2006), which crosscuts the major tectonic structures of central Morocco. This trend extends from the Siroua stratovolcano in the Anti-Atlas to the Mediterranean coast near Oujda (6.2 to 1.5 Ma, Tisserant et al. 1985, Andries and Bellon 1989; El Azzouzi et al. 1999; Duggen et al. 2005) and the Oran area in Algeria (4 to 0.8 Ma; Coulon et al. 2002). Gravimetric and geodetic modeling of the lithosphere suggests the role of an asthenospheric “hot lineament”, the so called Morocco Hot Line (MHL, e.g. Frizon de Lamotte et al. 2008 and references therein). This MHL could in fact extend from the Canary Islands to southeast Spain at least (e.g. Doblas et al. 2007; Duggen et al. 2009). According to available K-Ar ages (Harmand and Cantagrel 1984; Berrahma and Delaloye 1989; Berrahma et al. 1993; Morel and Bellon 1996; El Azzouzi et al. 1999, 2010), this volcanism was emplaced from the Miocene to the Quaternary (16.25 to 0.6-0.5 Ma). However, dykes and sills of lamprophyres, phonolites, nepheline syenites, nephelinites and carbonatites (Bouabdli et al. 1988; Mourtada et al. 1997) crosscutting the Tamazert alkaline intrusion (High Atlas) and its limestone country rocks gave older (Eocene) ages between 45 and 35 Ma (Bernard-Griffiths et al. 1991). Other Eocene K-Ar ages were reported for Rekkam basanites and nephelinites, with sixteen results clustered between 50 and 39 Ma and two younger ages at 35 and 32.5 Ma (Rachdi et al. 1997), and for the Zebzate nephelinite in the Middle Atlas (35 ± 3 Ma, Harmand and Cantagrel 1984).

The Middle Atlas basaltic province comprises the largest and youngest volcanic fields in Morocco. A hundred well-preserved strombolian cones and maars occur along a N-S trend ca. 70 km long between El Hajeb and Itzer (Fig. 1). Most of the volcanic units cap the flat karstic surface of a tabular Jurassic dolomitic limestone plateau (Martin 1981; Moukadiri 1983, 1999; Harmand and Moukadiri 1986). The latter overlies Triassic red beds and tholeiitic lava flows of the Central Atlantic Magmatic Province (CAMP) which in turn rest uncomformably over a Paleozoic basement. K-Ar ages (Harmand and Cantagrel 1984; Morel and Bellon 1996; El Azzouzi et al. 1999, 2010) show that the Middle Atlas volcanic activity occurred during the Miocene, the Pliocene and the Quaternary until 0.6-0.5 Ma. However, the occurrence of younger eruptions cannot be discarded given the excellent preservation of some volcanic landforms (deep maar craters, breached strombolian craters, tumuli and pressure ridges on the surface of pahoehoe lava flows). Some maar deposits (Tafraoute, Bou-Ibalrhatene; outlined in Fig. 1) contain abundant mantle xenoliths (spinel lherzolites, pyroxenites, garnet-bearing pyroxenites) as well as granulites from lower crust (Moukadiri 1983; 1999; Moukadiri and Kornprobst 1984; Moukadiri and Bouloton 1998; Moukadiri and Pin 1998). The Bou-Ibalrhatene xenolith suite includes metasomatic amphibole-bearing lherzolites and harzburgites, wehrlites, websterites, pyroxenites and hornblendites (Raffone et al. 2009; Wittig et al. 2009, 2010a, 2010b; Malarkey et al. 2011; Natali et al. 2013). Numerous basaltic flows, some of them 30 to 50 km long, were emitted from the strombolian cones. The total surface covered by the volcanics is rather large (960 km^2), but the corresponding estimated volume remains low (20 km^3) because of the limited thickness (usually 20 to 30 m) of the lava flow pile. The map shown in Figure 1 is partly based on the geomorphological study of Martin (1981), who provided excellent descriptions of volcanic landforms, on the geological maps of Azrou and El Hajeb (Du Dresnay and Suter 1975; Faure-Muret and Mesloub 2005) and the petrologic map of El Azzouzi et al. (2010). The N160-170°E trend defined by the main vents (Outgui, El Koudiate, Habri, Hebri, Bou Tagarouine, Tabourite, Tamarrakoït) is clearly oblique with respect to the main regional faults which trend N040°E (Tizi n'Trettène) to N050°E (North Middle Atlas Fault) (Charrière 1990). The volcanic cover is nearly continuous in the central part of the chain, between Azrou and Timahdite, where large lava fields flank the volcanic axis. Three important volcanic structures are located away from this central part (Fig 1): the J. Tamarrakoït in the south, and the El Koudiate and Outgui strombolian cones in the north. The pahoehoe lava flows emitted from the Outgui cone poured out over the Quaternary deposits of the Saïs plain close to Meknès. A number of small to very small volcanic edifices occur in the periphery of the main volcanic zone: Ariana and Tamahrart (W of El Koudiate), Ouaoussenfacht (E of El Koudiate), Lougnina and Am Laraïs (SE of Tamarrakoït), and Tabourite and Si Mguid (W of Timahdite village). Most of them are made of an ash and cinder cone and one (or a few) short lava flow(s) emitted from its crater.

Four types of mafic lavas are distinguished in the petrologic map (Fig. 1), based on a hundred major and trace element analyses (El Azzouzi et al. 2010). Intermediate and evolved compositions are lacking, a feature which contrasts with other Moroccan volcanic fields (Siroua and Saghro). Nephelinites (SiO_2 = 36–41%) usually form small strombolian cones and associated lava flows located along the borders of the volcanic plateau, and most of them were emplaced prior to the other petrologic types. The basanites (SiO_2 = 41–45%) are the youngest lava type, and make up most of the well preserved cones located between Azrou and Itzer. The corresponding lava flows generally overlie the alkali basalt flows. Alkali basalts (SiO_2 = 46–51%) represent the dominant petrographic type, and their fissural lava flows cover most of the plateau surface, especially to the east (Oued Guigou Valley) and the west (Oued Tigrigra Valley) of the main volcanic axis. They also form the large northern cone of J. Outgui, whose flows covered the Quaternary formations of the Saiss plain. Finally, subalkaline basalts, richer in silica than the former types (SiO_2 = 52%), make up the El Koudiate cone and associated 20 km long lava flows. According to available datings (Harmand and Cantagrel 1984; Morel and Bellon 1996; El Azzouzi et al. 1999), the Middle Atlas Miocene volcanic events emplaced only nephelinites, from 14.6 Ma (Bekrit) to 5.9 Ma (Talzast). However, nephelinites also erupted during the Quaternary, around 1.6 Ma (J. Tourguejid) and 0.75 Ma (J. Tahabrit). Alkaline and subalkaline basalts as well as basanites seem to be exclusively Quaternary in age, and the youngest published ages have been measured on basanites (0.8 Ma at J. Tahabrit, 0.6 Ma at J. Am Larais, 0.5Ma at J. Aït el Haj; see also the recent work of El Azzouzi et al. 2010 for more detail).

The alkali basalts, basanites and nephelinites display strongly enriched incompatible element patterns. Their geochemical signatures are typically intraplate alkaline, and hardly distinguishable from those of ocean island alkali basalts (OIB) and related rocks. The progressive enrichment in the most incompatible elements from alkali basalts to nephelinites, is consistent with decreasing degrees of partial melting of an enriched mantle source (El Azzouzi et al. 1999, 2010; Duggen et al. 2009). Isotopic data indicate an enriched mantle source, with almost no radiogenic Sr, showing rather variable Nd isotopic ratios, and consistently rich in radiogenic Pb (El Azzouzi et al. 1999; Duggen et al. 2009). This isotopic signature is close to the HIMU end-member recognized in oceanic islands such as St. Helens and Tubuai. Such a signature is frequently found in Cenozoic alkali basalts and basanites from Europe, the western Mediterranean, northern Africa, and eastern Atlantic islands (Madeira, Canary archipelago). These lavas are thought to derive from a 2500 to 4000 km large giant asthenospheric plume which would have ascended below these areas during the Early Tertiary (Hoernle et al. 1995).

The studied mantle xenoliths were taken in two volcanoes: the maar of Bou-Ibalrhatene (33°20'11.52"N - 5° 3'24.16"W) and the maar of Tafraoute (33°31'10.20"N - 4°41'37.60"W) that contain abundant mantle xenoliths (spinel lherzolites, pyroxenites) as well as granulites from lower crust (Fig. 1). The Bou-Ibalrhatene mantle xenolith suite that includes metasomatic amphibole-bearing lherzolites and harzburgites, wehrlites, websterites, clinopyroxenites and hornblendites have been widely studied (Moukadiri 1983, 1999; Moukadiri and Kornprobst 1984; Raffone et al. 2009; Wittig et al. 2009, 2010a, 2010b; Malarkey et al. 2011; Natali et al. 2013) while the Tafraoute mantle suite has been briefly described by Moukadiri (1983, 1999).

Petrographic outlines

All the investigated mantle xenoliths are lherzolites and harzburgites characterized by a protogranular to granular texture with grain size up to 6 mm. Moreover they contain, in particular the harzburgites, minor amounts of interstitial glass always surrounded by reaction rims. All the xenoliths are composed by four main primary minerals, olivine, orthopyroxene, clinopyroxene and very scarce spinel. All the olivine appears quite homogeneous in size (about 400-500 μm), slightly fractured and never altered. Orthopyroxene shows variable dimensions (about 100-600 μm) and only sometimes is characterized by the presence of exsolution lamellae. Clinopyroxene shows variable dimensions (in the range 50-400 μm) and is often fresh. Very rarely it is characterized by a spongy texture and by cleavages filled by indistinguishable oxides. Notably, these structures are homogeneously distributed and do not appear related to a contact with the interstitial glass.

Finally, spinels are quite uncommon, pale brown in colour and always smaller than 200 μm, idiomorphic and located inside primary olivine or orthopyroxene crystals.

The blebs of glass are variably concentrated in the mantle xenoliths and appear to be aligned along preferential directions. All the blebs are surrounded by reaction rims where small crystals represented by clinopyroxene, orthopyroxene and very rare amphibole can be recognized as phases belonging to a secondary generation.

Experimental procedures

Nine spinels have been analyzed by means of X-ray diffraction and electron microprobe. X-ray diffraction data were collected on an automated KUMA-KM4 (K-geometry) diffractometer, using MoKα radiation, monochromatized by a flat graphite crystal. Data was collected, according to Della Giusta et al. (1996), with up to 55° of 2θ in the ω-2θ scan mode (scan width 1.8° 2θ, counting times from 20 to 50 s, depending on the peak standard deviation). Twenty-four equivalent reflections of 12 8 4 or 8 4 4 peaks (according to the size of the Cr-spinel), at about 80° or 50° of 2θ, respectively, were accurately centered at both sides of 2θ, and the α_1 peak barycenter was used for cell parameter determination. Corrections for absorption were performed according to North et al. (1968). Structural refinement using the SHELX-97 program (Sheldrick 2008) was carried out against Fo^2_{hkl} in the Fd–3m space group (with the origin at –3m), since no evidence of different symmetry appeared. Scattering factors were taken from Prince (2004) and Tokonami (1965). The crystallographic data are presented in Table 1.

Ten to fifteen spot analyses were performed on the same Cr-spinels used for X-ray data collection, using a CAMECA-CAMEBAX electron microprobe operating at 15 kV and 15 nA. A 20 s counting time was used for both peak and total background. Synthetic oxide standards (MgO, FeO, MnO, ZnO, NiO, Al_2O_3, Cr_2O_3 and TiO_2) were used. Raw data were reduced by PAP-type correction software provided by CAMECA. The mineral chemical analyses are reported in Table 2.

The cation distribution (Table 2) between the T and M sites was obtained with the method described by Carbonin et al. (1996) and Lavina et al. (2002), in which crystal chemical parameters are calculated as a function of the atomic fractions at the two sites and fitted to the observed values. Site atomic fractions were calculated by minimizing the function F(x) (Table 2), which takes into account the mean of the square differences between calculated and observed parameters divided by their squared standard deviations.

Results

Cell edges are usually within the range 8.13-8.14 Å, but there are three samples with longer *a* value, so that the whole analyzed spinels are within the range 8.1334 (4) – 8.2021 (2) Å, while the oxygen positional parameter is very similar ranging between 0.2626 (1) and 0.2629 (2) (Table 1). These values are rather common for spinels from mantle xenoliths as it can be seen in Figure 2 where the here studied spinels are compared with other mantle xenoliths (Della Giusta et al. 1986; Princivalle et al. 1989; Carraro 2003; Uchida et al. 2005; Nédli et al. 2008) and peridotite massif occurrences showing higher *u* values for similar cell edges (Ivrea-Verbano zone, Basso et al. 1984; Ronda, Lenaz et al. 2010).

From a chemical point of view the most variable oxides are the trivalent Al_2O_3 and Cr_2O_3 that ranges between 36 and 56 wt.% (1.205-1.713 atoms per formula unit, apfu) and 9.6 to 30 wt. % (0.197-0.664 apfu), respectively. MgO and iron oxides, both FeO and Fe_2O_3, show narrow ranges being comprised between 17-21 wt.% (0.731-0.813 apfu), 8-11 wt.% (0.174-0.258) and 4-6 wt.% (0.077-0.125 apfu) , respectively. As regards the minor oxides NiO is lower than 0.4 wt.%, TiO_2 is comprised between 0.1 and 0.2 while MnO and ZnO are lower than 0.13.

The inversion degree is limited, i.e. the amount of trivalent cations present in T site and of the divalent cations in M site, with less than 0.2 apfu of trivalent cation in the tetrahedral site.

Intracrystalline closure temperatures calculated by using the Princivalle et al. (1999) geothermometer are in the range 550-750°C. This geothermometer takes into account the Mg- and Al-content of the Cr-spinels and their distribution among the octahedral and tetrahedral sites. The presence of other cations is accounted for by coefficients present in the equation of the geothermometer.

Discussion and conclusions

As mentioned above, the structural parameters of the present spinels show relevant variations in unit cell values and insignificant variations in *u* parameters. Previous studies showed that large variations in trivalent cations, especially Cr, are the most responsible of variations in the cell edges and this fact is not restricted to the mantle xenoliths occurrences but also to Cr-spinels and chromites from layered complexes (Lenaz et al. 2007, 2011, 2012), ophiolites (Derbyshire et al. 2013), komatiites (Lenaz et al. 2004a), kimberlites and diamond inclusions (Lenaz et al. 2009). As far as concern the mantle xenoliths this fact can be easily recognized in Figure 3, where the Moroccan spinels are compared with other mantle xenoliths worldwide (Della Giusta et al. 1986; Princivalle et al. 1989; Carraro 2003; Uchida et al. 2005; Nédli et al. 2008; Princivalle et al., 2014). The most peculiar geometrical parameter, in spinels from mantle xenoliths, is *u*. In fact, as previously noted by Princivalle et al. (1989) it is characteristic of each suite of mantle xenoliths. In the case of the Moroccan xenoliths the average value is 0.2628 (1) for the BI and the TF samples as well, while it is 0.2624 (1) for Mt. Leura, 0.2625 (1) for NE Brazil and Mt. Noorat, 0.2627 (1) for Assab (Princivalle et al. 1989), 0.2628 (1) for Predazzo (Carraro 2003) and 0.2629 (1) for San Carlos (Arizona; Uchida et al. 2005). As the *u* values of each suite is more or less constant, those authors related the *u* values of the mantle xenoliths spinels to their cooling history. On the contrary, all the other occurrences show that the *u* values too, are mainly related to the chemistry of the spinels. An interesting fact came out from the analyses and comparisons of the intracrystalline closure temperatures (Fig. 4). For Moroccan samples they are rather low, in the range 550-750°C, comparable only with spinels from Hannuoba (China; Princivalle et al., 2014), while for all the other occurrences they are higher than 730°C (minimum temperature recorded in Predazzo spinels; Carraro 2003). It is supposed that the intracrystalline closure temperature of the spinels is that recorded in the mantle and it is not conditioned by the temperature of the ascending magma, i.e. no re-equilibration occurs. Considering this, why is the temperature of the Moroccan spinels so low in comparison with the others? As these temperatures are related to the cooling history of the spinels themselves and to the oxygen positional parameter we can suppose that the cooling was similar to that of the other mantle xenoliths having comparable inversion degree. The oxygen positional parameter is similar to that of other spinels from mantle xenoliths considered having higher intracrystalline closure temperature. Given that, having similar cooling history but different intracrystalline temperature, we suppose that below the West Africa Craton, when the spinels formed, the mantle possibly had temperature lower of those of the other considered xenoliths, even if actually this area is characterized by a high geothermal gradient (Rimi 2001) and tomographic data suggest that the underlying asthenospheric mantle is anomalously hot (Spakman et al. 1993; De Jonge et al. 1994; Hoernle et al. 1995; Goes et al. 1999). Moreover, it is interesting to notice that spinels from Ronda has higher *u* values (Fig. 5) but, for those with similar Cr contents the same intracrystalline closure temperatures. Lenaz et al. (2010) noticed that the intracrystalline closure temperature seem to be reached faster for Cr-spinels in mantle xenoliths and is usually higher than that of Cr-spinels in mantle peridotite and associated dikes. At now, we have the evidence of two occurrences possibly derived from almost the same mantle. The Ronda massif emplaced in Early Miocene times being exhumed from about 66 km depths (Platt et al. 2003). According to the mantle diapir model (Obata 1980), the Ronda peridotite is interpreted in terms of an ascending hot, slowly cooling peridotite mass, where the spinel tectonites represent an old lithospheric mantle, isolated from the convective mantle at 1.36 Ga (Reisberg and Lorand 1995). Lenaz et al. (2010) noticed that the intracrystalline temperatures of Ronda spinels is about 0-150°C lower than the intercrystalline temperature calculated by Li et al. (1995) by using the olivine-spinel thermometer and the same is also for chromite samples from Oman (unpublished data), disseminated spinels in peridotite from Rum Island show intra- and inter-crystalline temperatures that are comparable (Lenaz et al. 2011). Given that we can assume that the intercrystalline temperature for the here studied occurrences are in the range 600-850°C. Considering the behavior of some geotherms found in the literature, like the Catalonia or the SE Australia, the assumed temperatures (600-850°C) are confined in a depth of about 20-40 Km (Puziewicz et al. 2012). Lithospheric models proposed by Teixell et al. (2005) for the studied area indicate that the lower crust reaches its deepest value in a range between 30 and 40 Km. Consequently, we can assume that the here studied xenoliths were emplaced at a “shallow” depth of about 20-40 Km, just beneath the lower crust, where they were disrupted and brought to the surface from the ascending alkaline lavas together with some crustal xenoliths similarly to what happened also in Hannuoba (China; Princivalle et al., 2014).

Implications from this study

Mantle xenoliths, as well as, other mafic and ultramafic rocks are mainly constituted by olivines ± pyroxenes that are usually subjected to different degrees of alteration and weathering. As an example, Ahmed et al. (2005) and Sobolev and Logvinova (2005) pointed out that, in many cases, ultramafic rocks including kimberlite, lamproite, and peridotite of orogenic massifs are heavily serpentinized and that such alterations present difficulties in identifying the presence of olivine and pyroxene, and the same is also true for ophiolite occurrences (Lenaz et al. 2000, and references therein). On the contrary, Cr-bearing spinel may be present as the sole-surviving primary mineral. This implies that even in the case of a mantle xenoliths where all the silicates could be heavily altered, the presence of one single crystal of Cr-spinel and the study of its oxygen coordinates (*u*), inversion parameters (*i*), Cr content, and calculated closure temperatures can be used to validate the thermal history of the mantle xenoliths. The combined approach of structural data, intra- and inter-crystalline temperatures and the geophysical data seems to be an interesting tool to assess the pre-exhumation history of the mantle xenoliths.

Acknowledgements

The Italian C.N.R. financed the installation and maintenance of the microprobe laboratory in Padova. L. Furlan, R. Carampin and L. Tauro are kindly acknowledged for technical support. DL would like to thanks the PRIN 2010-11 fund (SPIN GEO TECH). RA Fregola and an anonymous referee are kindly acknowledged for their comments.

References

Ahmed, A.H., Arai, S., Abdel-Aziz, Y.M., and Rahimi, A. (2005) Spinel composition as a petrogenetic indicator of the mantle section in the Neoproterozoic Bou Azzer ophiolite, Anti-Atlas, Morocco. Precambrian Research, 138, 225–234.

Andries, D. and Bellon, H. (1989) Ages isotopiques ^{40}K-^{40}Ar du volcanisme alcalin néogène d'Oujda (Maroc oriental) et implications tectoniques. Sciences Géologique Mémoires (Strasbourg), 84, 107-116.

Basso, R. Comin-Chiaramonti, P. Della Giusta, A. and Flora, O. (1984) Crystal chemistry of four Mg-Fe-Al-Cr spinels from the Balmuccia peridotite (Western Italian Alps). Neues Jahrbuch für Mineralogie Abhandlungen, 150, 1–10.

Beccaluva, L., Azzouni-Sekkal A., Benhallou A., Bianchini G., Ellam R.M., Marzola M., Siena F. and Stuart F.M. (2007) Intracratonic asthenosphere upwelling and lithosphere rejuvenation beneath the Hoggar swell (Algeria): Evidence from HIMU metasomatised lherzolite mantle xenoliths. Earth and Planetary Science Letters, 260, 482-494.

Beccaluva L., Bianchini G., Ellam R.M., Marzola M., Oun K.M., Siena F. and Stuart F.M., 2008. The role of HIMU metasomatic components in the African lithospheric mantle: petrological evidence from the Gharyan peridotite xenoliths, NW Libya. In M. Coltorti, M. Grégoire (Eds.) Mantle metasomatism in intra-plate and suprasubduction settings. Geological Society, Special Publication, 293, 253-277

Bernard-Griffiths, J. Fourcade, S. and Dupuy, C. (1991) Isotopic study (Sr, Nd, O and C) of lamprophyres and associated dykes from Tamazert (Morocco): crustal contamination process and source characteristics. Earth and Planetary Science Letters, 103, 190-199.

Berrahma, M. and Delaloye, M. (1989) Données géochronologiques nouvelles sur le massif volcanique du Siroua (Anti-Atlas, Maroc). Journal of African Earth Science, 9, 651-656.

Berrahma, M. Delaloye, M. Faure-Muret, A. and Rachdi, H. E. N. (1993) Premières données géochronologiques sur le volcanisme alcalin du Jbel Saghro, Anti-Atlas, Maroc. Journal of African Earth Science, 17, 333-341.

Bosi, F. Andreozzi, G.B. Ferrini, V. and Lucchesi, S. (2004) Behavior of cation vacancy in kenotetrahedral Cr-spinels from Albanian eastern belt ophiolites. American Mineralogist, 89, 1367–1373.

Bouabdli, A. Dupuy, C. Dostal, J. (1988) Geochemistry of Mesozoic alkaline lamprophyres and related rocks from the Tamazert massif, High Atlas (Morocco). Lithos, 22, 43–58.

Carbonin, S. Russo, U. and Della Giusta, A. (1996) Cation distribution in some natural spinels from X-ray diffraction and Mössbauer spectroscopy. Mineralogical Magazine, 60, 355–368.

Carbonin, S. Menegazzo, G. Lenaz D. and Princivalle, F. (1999) Crystal chemistry of two detrital Cr-spinels with unusual low values of oxygen positional parameter: oxidation mechanism and possible clues to their origin. Neues Jahrbuch für Mineralogie Monatshefte, 359–371.

Carraro, A. (2003) Crystal chemistry of Cr-spinels from a suite of spinel peridotite mantle xenoliths from the Predazzo Area (Dolomites, Northern Italy). European Journal of Mineralogy, 15, 681–688.

Charrière, A. (1990) Héritage Hercynien et évolution géodynamique alpine d'une chaîne intracontinentale: le Moyen Atlas au sud-est de Fès (Maroc). Thèse Doctorat d'Etat, Toulouse, 559 p.

Coulon, C. Megartsi, M. Fourcade, S. Maury, R.C. Bellon, H. Louni-Hacini, A. and Cotton, J. (2002) Post-collisional transition from calc-alkaline to alkaline volcanism during the Neogene in Oranie (Algeria): magmatic expression of a slab breakoff. Lithos, 62, 87-110.

De Jonge, M.R. Wortel, M.J.R. and Spakman, W. (1994) Regional scale tectonic evolution and the seismic velocity structure of the lithosphere and upper mantle: the Mediterranean region. Journal of Geophysical Research, 99, 12091-12108.

Della Giusta, A., Princivalle, F. and Carbonin, S. (1986) Crystal chemistry of a suite of natural Cr-bearing spinels with $0.15<Cr<1.07$. Neues Jahrbuch für Mineralogie Abhandlungen, 155, 319–330.

Della Giusta, A. Carbonin, S. and Ottonello, G. (1996) Temperature-dependent disorder in a natural Mg–Al–Fe^{2+}–Fe^{3+} – spinel. Mineralogical Magazine, 60, 603–616.

Derbyshire, E.J. O'Driscoll, B. Lenaz, D. Gertisser, R. and Kronz, A. (2013) Compositionally heterogeneous podiform chromitite in the Shetland Ophiolite Complex (Scotland):

Implications for chromitite petrogenesis and late-stage alteration in the upper mantle portion of a supra-subduction zone ophiolite. Lithos, 162-163, 279-300.

Doblas, M., López-Ruiz, J. and Cebriá, J.M. (2007) Cenozoic evolution of the Alboran Domain : A review of the tectonomagmatic models. In : Beccaluva, L., Bianchini, G. and Wilson, M. (eds.) GSA Special Papers 418, Cenozoic Volcanism in the Mediterranean Area, 303-320.

Du Dresnay, R. and Suter, G. (1975) Carte géologique du Maroc au 1/100 000 : El Hajeb. Notes et Mémoires Service Géologique Maroc, no 160.

Duggen, S. Hoernle, K. Van Den Bogaard, P. and Garbe-Schönbrg, A. (2005) Post-collisional transition from subduction to intraplate-type magmatism in the westernmost Mediterranean: evidence for continental-edge delamination of subcontinental lithosphere. Journal of Petrology, 46, 1155-1201.

Duggen, S. Hoernle, K.A. Hauff, F. Klügel, A. Bouabdellah, M. and Thirlwall, M.F. (2009) Flow of Canary mantle plume material through a subcontinental lithospheric corridor beneath Africa to the Mediterranean. Geology, 37, 283-286.

El Azzouzi, M. Bernard-Griffiths, J. Bellon, H. Maury, R.C. Pique, A. Fourcade, S. Cotten J. and Hernandez, J. (1999) Evolution des sources du volcanisme marocain au cours du Néogène. Comptes Rendus de L'Academie des Sciences, 329, 95-102.

El Azzouzi, M. Maury, R.C. Bellon, H. Youbi, N. Cotten, J. and Kharbouch, F. (2010) Petrology and K-Ar chronology of the Neogene-Quaternary Middle Atlas basaltic province, Morocco. Bullettin Societe Geologique France, 181, 243-257.

El Bakkali, S. Gourgaud, A. Bourdier, J.-L. Bellon, H. and Gundogdu, N. (1998) Post-collision Neogene volcanism of the eastern Rif (Morocco): magmatic evolution through time. Lithos, 45, 523-543.

Faure-Muret, A. and Mesloub, S. (2005) Carte géologique du Maroc (1/50 000), feuille d'Azrou. – Notes et Mémoires Service Géologique Maroc, no 461.

Frizon De Lamotte, D. Crespo-Blanc, A. Saint-B'Ezar, B. Comas, M. Fernandez, M. Zeyen, H. Ayarza, H. Robert-Charrue, C. Chalouan, A. Zizi, M. Teixell, A. Arboleya, M.L. Alvarez-Lobato, F. Julivert, M. Michard, A. (2004) TRANSMED-transect I : Betics, Alboran Sea, Rif, Moroccan Meseta, High Atlas, Jbel Saghro, Tindouf Basin, in Cavazza W. Roure F. SpakmanW. Stampfli G.M. Ziegler P.A. (Eds.), The TRANSMED Atlas – the Mediterranean region from crust to mantle, Springer, Berlin, pp. 91–96.

Frizon De Lamotte, D.Zizi, M.Missenard, Y. Hafid, M. El Azzouzi, M. Maury, R.C. Charrière, A. Taki, Z. Benammi, M. and Michard, A. (2008) – Chapt. 4: The Atlas system. In : A. Michard, O. Saddiqi, A. Chalouanand D. Frizon De Lamotte, Eds. Continental evolution: the geology of Morocco. Structure, stratigraphy and tectonics of the Africa-Atlantic-Mediterranean triple junction. – Lecture Notes in Earth Sciences, 116, Springer-Verlag, Berlin, Heidelberg, 133-202.

Goes, S. Spakman, W. and Bijwaard, H. (1999) A lower mantle source for Central European volcanism. Science, 286, 1928-1931.

Harmand, C. and Cantagrel, J.M. (1984) Le volcanism alcalin Tertiaire et Quaternaire du Moyen Atlas (Maroc): chronologie K/Ar et cadre géodinamique. Journal of African Earth Sciences, 2, 51-55.

Harmand, C. Moukadiri, A. (1986) Synchronisme entre tectonique compressive et volcanisme alcalin: exemple de la province Quaternaire du Moyen Atlas (Maroc). Bulletin de la Société Géologique de France, 4, 595-603.

Hernandez, J. and Bellon, H. (1985) Chronologie K-Ar du volcanisme miocène du Rif oriental (Maroc): implications tectoniques et magmatologiques. Rev. Géol. Dyn. Géogr. Phys. 26, 2, 85-94.

Hernandez, J. Larouziere, F.D. de, Bolze, J. and Bordet, P. (1987) Le magmatisme néogène bético-rifain et le couloir de décrochement trans-Alboran. Bulletin de la Société Géologique de France, 8, 257-267.

Hill, R.J. Craig, J.R. and Gibbs, G.V. (1979) Systematics of the spinel structure type. Physics and Chemistry of Minerals, 4, 317-339.

Hoernle, K. Zhang, Y.S. and Graham, D. (1995) Seismic and geochemical evidence for large-scale mantle upwelling beneath the eastern Atlantic and western and central Europe. Nature, 374, 34-39.

Lavina, B. Salviulo, G. and Della Giusta, A. (2002) Cation distribution and structure modeling of spinel solid solutions. Physics and Chemistry of Minerals, 29,10–18.

Lenaz, D. and Lughi, V. (2013) Raman study of $MgCr_2O_4$–$Fe^{2+}Cr_2O_4$ and $MgCr_2O_4$–$MgFe_2^{3+}O_4$ synthetic series: the effects of Fe^{2+} and Fe^{3+} on Raman shifts. Physics and Chemistry of Minerals, 40, 491-498.

Lenaz, D. and Princivalle, F. (1996) Crystal-chemistry of detrital chromites in sandstones from Trieste (NE Italy). Neues Jahrbuch für Mineralogie Monatshefte, 429–434.

Lenaz, D. and Princivalle, F. (2005) The crystal chemistry of detrital chromian spinel from the southeastern Alps and Outer dinarides: The discrimination of supplies from areas of similar tectonic setting? Canadian Mineralogist, 43, 1305-1314.

Lenaz, D. and Skogby, H. (2013) Structural changes in the $FeAl_2O_4$–$FeCr_2O_4$ solid solution series and their consequences on natural Cr-bearing spinels. Physics and Chemistry of Minerals, 40, 587-595.

Lenaz, D., Kamenetsky, V.S., Crawford, A.J., Princivalle, F. (2000) Melt inclusions in detrital spinels from the SE Alps (Italy-Slovenia): A new approach to provenance studies of sedimentary basins. Contributions to Mineralogy and Petrology, 139, 748-758.

Lenaz, D. Carbonin, S. Gregorić, M. and Princivalle, F. (2002) Crystal chemistry and oxidation state of one euhedral Cr-spinel crystal enclosed in a bauxite layer (Trieste Karst: NE Italy): some considerations on its depositional history and provenance. Neues Jahrbuch für Mineralogie Monatshefte, 193–206.

Lenaz, D. Andreozzi, G.B. Mitra, S. Bidyananda, M. and Princivalle, F. (2004a) Crystal chemical and ^{57}Fe Mössbauer study of chromite from the Nuggihalli schist belt (India). Mineralogy and Petrology, 80, 45–57.

Lenaz, D. Skogby, H. Princivalle, F. and Hålenius, U. (2004b) Structural changes and valence states in the $MgCr_2O_4$ - $FeCr_2O_4$ solid solution series. Physics and Chemistry of Minerals, 31, 633-642.

Lenaz, D. Skogby, H. Princivalle, F. and Hålenius, U. (2006) The $MgCr_2O_4$–$MgFe_2O_4$ solid solution series: effects of octahedrally coordinated Fe^{3+} on T–O bond lengths. Physics and Chemistry of Minerals, 33, 465-474.

Lenaz, D. Braidotti, R. Princivalle, F. Garuti, G. and Zaccarini, F. (2007) Crystal chemistry and structural refinement of chromites from different chromitite layers and xenoliths of the Bushveld Complex. European Journal of Mineralogy, 19,599–609.

Lenaz, D. Logvinova, A.M. Princivalle, F. and Sobolev, N.V. (2009) Structural parameters of chromite included in diamonds and kimberlites from Siberia: a new tool for discriminating ultramafic source. American Mineralogist, 94, 1067–1070.

Lenaz, D. De Min, A. Garuti, G. Zaccarini, F. and Princivalle, F. (2010) Crystal chemistry of Cr-spinels from the lherzolite mantle peridotite of Ronda (Spain). American Mineralogist, 95,1323–1328.

Lenaz, D. O'Driscoll, B. and Princivalle, F. (2011) Petrogenesis of the anorthosite-chromitite association: crystal-chemical and petrological insights from the Rum Layered Suite, NW Scotland. Contributions to Mineralogy and Petrology, 162,1201–1213.

Lenaz, D. Garuti, G. Zaccarini, F. Cooper, R.W. and Princivalle, F. (2012) The Stillwater Complex chromitites: the response of chromite crystal chemistry to magma injection. Geologica Acta, 10, 33-41.

Lenaz, D. Skogby, H. Logvinova, A.M. Sobolev, N.V. and Princivalle, F. (2013) A micro-Mössbauer study of chromites included in diamond and other mantle-related rocks. Physics and Chemistry of Minerals, in press, DOI 10.1007/s00269-013-0602-8.

Li, J.-P., Kornprobst, J., and Vielzeuf, D. (1995) An improved experimental calibration of the olivine-spinel geothermobarometer. Chinese Journal of Geochemistry 14: 68-77.

Malarkey, J. Wittig, N. Pearson, D.G. and Davidson, J.P. (2011) Characterising modal metasomatic processes in young continental lithospheric mantle: a microsampling isotopic and trace element study on xenoliths from the Middle Atlas Mountains, Morocco. Contributions to Mineralogy and Petrology, 162, 289-302.

Martin J. (1981) – Le Moyen Atlas Central: étude géomorphologique. – Notes et Mémoires Service Géologique Maroc, no 258 bis, 445 p.

Maury, R.C. Fourcade, S. Coulon, C. El Azzouzi, M. Bellon, H. Coutelle, A. Ouabadi, A. Semroud, B. Megartsi, M.Cotton, J. Belanteur, O. Lounni-Hacini, A. Piqué, A. Capdevila, R. Hernandez, J. and Rehault, J.-P. (2000) Post-collisional Neogene magmatism of the Mediterranean Maghreb margin: a consequence of slab breakoff. Comptes Rendus de l'Academie des Sciences Paris, II, 331 (3), série II, 159-173.

Missenard, Y. Zeyen, H. Frizon de Lamotte, D. Leturmy, P. Petit, C. Sebrier, M. and Saddiqi, O. (2006) Crustal versus asthenospheric origin of relief of the Atlas Mountains of Morocco. Journal of Geophysical Research, 111, B03401, doi: 10.129/2005JB003708.

Morel, J.-M. and Bellon, H. (1996) Le volcanisme quaternaire du plateau d'Azrou, Maroc. Contribution à la datation isotopique des magmas associés. 13ème Colloque des bassins sédimentaires marocains, Univ. Cadi Ayyad, Marrakech, 19-22 Mars 1996, Résumé, 113.

Moukadiri, A. (1983) Les enclaves ultrabasiques assocées aux basaltes alcalins dans le district volcanique d'Azrou–Timahdit (Moyen Atlas, Maroc).:150. Thèse 3ème cycle, Université Blaise-Pascal, Clermont-Ferrand.

Moukadiri, A. (1999) Essai de caractérisation de la lithosphère sous le moyen Atlas (Maroc) par l'étude des Xénolites basi-crustaux et mantelliques dans les basaltes alcalins quaternaires. – Thèse Doctorat d'Etat, Université Cadi Ayyad, Faculté des Sciences-Semlalia, Marrakech

Moukadiri, A. and Bouloton, J. (1998) Pétrologie des granulites exhumées par le volcanisme récent du Moyen Atlas: aperçu sur la croûte inférieure néogène du Maroc central. Comptes rendus de l'Académie des sciences. Série 2. Sciences de la terre et des planètes, 327, 731-734.

Moukadiri, A. and Kornprobst, J (1984) Garnet and/or spinel bearing pyroxenites in alkali basalts near Azrou (Middle Atlas, Morocco): mantle derived alumina-rich xenoliths related to the 'ariegite–grospydite' trend. In: Kornprobst J, editor. Kimberlites II: The Mantle and Crust Relationship. Amsterdam: Elsevier; p. 179-189.

Moukadiri, A. and Pin, C. (1998) Géochimie (éléments majeurs et terres rares) des granulites méta-sédimentaires en xénolithes dans les basaltes alcalins quaternaires du Moyen Atlas (Maroc) : arguments en faveur de la nature pour partie restitique de la croûte inférieure. Comptes rendus de l'Académie des sciences. Série 2. Sciences de la terre et des planètes, 327, 589-595.

Mourtada, S. Le Bas, M.J. and Pin, C. (1997) Pétrogenèse des magnésio- carbonatites du complexe de Tamazert (Haut Atlas marocain). Comptes rendus de l'Académie des sciences. Série 2. Sciences de la terre et des planètes, 325, 559-564.

Natali, C., Beccaluva, L., Bianchini, G. Ellam, R.M., Siena, F. and Stuart, F.M. (2013) Carbonated alkali-silicate metasomatism in the North Africa lithosphere: Evidence from Middle Atlas spinel-lherzolites, Morocco. Journal of South American Earth Sciences, 113-121.

Nédli, Zs. Princivalle, F. Lenaz, D. and Tóth, T.M. (2008) Crystal chemistry of clinopyroxene and spinel from mantle xenoliths hosted in Late Mesozoic lamprophyres (Villány Mts, S Hungary). Neues Jahrbuch für Mineralogie Abhandlungen, 185, 1–10.

North, A.C.T. Phillips, D.C. and Scott-Mattews, F. (1968) A semi-empirical method of absorption correction. Acta Crystallographica, A24, 351–352.

Obata, M. (1980) The Ronda peridotite garnet-lherzolite, spinel-lherzolite, and plagioclase-lherzolite facies and the P-T trajectories of a high-temperature mantle intrusion. Journal of Petrology, 21, 533–572.

Platt, J.P. Argles, T.W. Carter, A. Kelley, S.P. Whitehouse, M.J. and Lonergan, L. (2003) Exhumation of the Ronda peridotite and its crustal envelope: constraints from thermal modeling of a P-T-time array. Journal of the Geological Society, 160, 655–676.

Prince, E. (2004) International Tables for X-ray Crystallography. Volume C: Mathematical, Physical and Chemical Tables, 3rd ed. Springer, Dordrecht, The Netherlands.

Princivalle, F. Della Giusta, A. and Carbonin, S. (1989) Comparative crystal chemistry of spinels from some suites of ultramafic rocks. Mineralogy and Petrology, 40, 117–126.

Princivalle, F. Della Giusta, A. De Min, A. and Piccirillo, E.M. (1999) Crystal chemistry and significance of cation ordering in Mg–Al rich spinels from high-grade hornfels (Predazzo-Monzoni, NE Italy). Mineralogical Magazine, 63, 257–262.

Princivalle, F., De Min, A., Lenaz, D., Scarbolo, M., Zanetti, A. (2014) Ultramafic xenoliths from Damaping (Hannuoba region, NE-China): Petrogenetic implications from crystal chemistry of pyroxenes, olivine and Cr-spinel and trace element content of clinopyroxene. Lithos, in press.

Puziewicz, J., Czechowski, L., Krysiński, L., Majorowicz, J., Matusiak-Małek, M., Wróblewska, M. (2012) Lithosphere thermal structure at the eastern margin of the Bohemian Massif: a case petrological and geophysical study of the Niedźwiedź amphibolite massif (SW Poland). International Journal of Earth Sciences, 101, 1211-1228.

Rachdi, H. N. Berrahma, M. Delaloye, M. Faure-Muret, A. and Dahmani, M. (1997) Le volcanisme tertiaire du Rekkame (Maroc): pétrologie, géochimie et géochronologie. Journal of African Earth Sciences, 24, 3, 259-269.

Raffone, N. Chazot, G. Pin, C. Vannucci, R. and Zanetti, A. (2009) Metasomatism in the lithospheric mantle beneath Middle Atlas (Morocco) and the origin of Fe- and Mg-rich wehrlites. Journal of Petrology, 50, 197-249.

Reisberg, L. and Lorand, J.P. (1995) Longevity of sub-continental mantle lithosphere from osmium isotope systematics in orogenic peridotite massifs. Nature, 376, 159–162.

Rimi, A. (2001) Carte du gradient géothermique au Maroc. Bullettin Institute Scientifique Rabat, 23, 1-6.

Sheldrick, G.M. (2008) A short history of SHELX. Acta Crystallographica, A64, 112-122.

Sobolev, N.V. and Logvinova, A.M. (2005) Significance of accessory chrome spinel in identifying serpentinite paragenesis. International Geology Review, 47, 58–64.

Spakman, W. Van der Lee, S. and Van der Hilst, R. (1993) Travel-time tomography of the European-Mediterranean mantle down to 1400 km. Physics of the Earth and Planetary Interiors, 79, 3-74.

Teixell, A., Ayarza, P. Zeyen, H. Fernandez, M. and Arboleya, M.-L. (2005) Effects of mantle upwelling in a compressional setting: the Atlas Mountains of Morocco. Terra Nova, 17, 456-461.

Tisserant, D., Laouina, A. and Clauer, P. (1985) Datation K/Ar des basaltes de la plaine d'Angad. Sciences Géologiques Bulletin, 38, 2,114-145.

Tokonami, M. (1965) Atomic scattering factor for O^{-2}. Acta Crystallographica, 19, 486.

Uchida, H., Lavina, B. Downes, R.T. and Chesley, J. (2005) Single-crystal X-ray diffraction of spinels from the San Carlos Volcanic Field, Arizona: Spinel as a geothermometer. American Mineralogist, 90, 1900–1908.

Wittig, N., Pearson, D.G., Downes, H. and Baker, J.A. (2009) The U, Th and Pb elemental and isotope compositions of mantle clinopyroxenes and their grain boundary contamination derived from leaching and digestion experiments. Geochimica et Cosmochimica Acta, 73, 469-488.

Wittig, N., Pearson, D.G. Baker, J.A. Duggen, S. Hoernle, K. (2010a) A major element, PGE and Re–Os isotope study of Middle Atlas (Morocco) peridotite xenoliths: evidence for coupled introduction of metasomatic sulphides and clinopyroxene. Lithos, 115,15–26.

Wittig, N., Pearson, D.G., Baker, J.A., Duggen, S., and Hoernle, K. (2010b) Tracing the metasomatic and magmatic evolution of continental mantle roots with Sr, Nd, Hf and Pb isotopes: a case study of Middle Atlas (Morocco) peridotite xenoliths. Geochimica et Cosmochimica Acta, 74, 1417–1435.

Zeyen, H. Ayarza, P. Fernandez, M. and Rimi, A. (2005) Lithospheric structure under the western African-European plate boundary: a transect across the Atlas Mountains and the Gulf of Cadiz. Tectonics, 24, TC2001, 1-16, doi: 10.129/2004TC001639.

Figures captions

Figure 1. Simplified geologic map of Middle Atlas Volcanic Field showing the distribution of the four petrographic types (El Azzouzi et al. 2010). Inset: Main tectonic structures of Morocco, location of the Middle Atlas and distribution of Neogene and Quaternary volcanism.

Figure 2. Oxygen positional parameter, *u*, vs. cell edge, *a*. Full circle: BI samples (this study); full diamond: TF samples (this study). Mantle xenoliths, open square: Mt. Leura (Della Giusta et al. 1989); open triangle: NE Brazil (Princivalle et al. 1989); open diamond: Assab (Princivalle *et al*. 1989); cross: Mt. Noorat (Princivalle et al. 1989); asterisk: Predazzo (Carraro, 2003); open circle: San Carlos (Uchida et al. 1989); plus: Hungary (Nédli et al. 1989). Peridotite massif, full triangle: Balmuccia (Della Giusta et al. 1986), full square: Ronda (Lenaz et al. 2010).

Figure 3. Cell edge, a, vs. Cr content in atoms per formula unit (apfu). Full diamond: this study. Mantle xenoliths, open square: Mt. Leura (Della Giusta et al. 1989); open triangle: NE Brazil (Princivalle et al. 1989); open diamond: Assab (Princivalle *et al*. 1989); cross: Mt. Noorat (Princivalle et al. 1989); asterisk: Predazzo (Carraro, 2003); open circle: San Carlos (Uchida et al. 2005); plus: Hungary (Nédli et al. 2008). Peridotite massif, full triangle: Balmuccia (Della Giusta et al. 1986), full square: Ronda (Lenaz et al. 2010). Error bars within the symbols.

Figure 4. Range of intracrystalline closure temperatures for the studied spinels and mantle xenoliths used for comparison (Mt. Leura, Della Giusta et al. 1989; Mt. Noorat, NE Brazil, Assab, Princivalle et al. 1989; San Carlos, Uchida et al. 2005; Predazzo, Carraro 2003; Hannuoba, unpublished data).

Figure 5. Oxygen positional parameter, *u*, vs. intracrystalline closure temperatures of mantle xenoliths worldwide and peridotite massif. Symbols as in Figure 3.

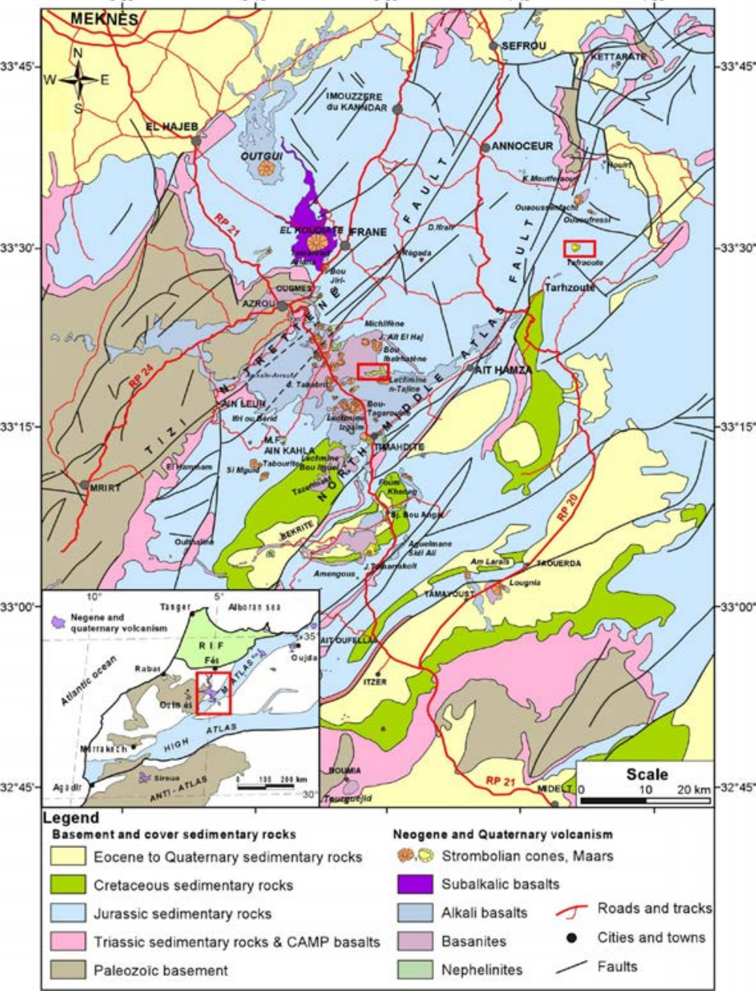

5°30'
5°15'
5°00'
4°45'
4°30'
33°45'
33°30'
33°15'
33°00'
32°45'
MEKNES
SEFROU
KETTARATE
IMOUZZERE du KANNDAR
EL HAJEB
ANNOCEUR
OUTGUI
EL KOUDIATE
IFRANE
RP 21
FAULT
D.Ifrah
Tafraoute
Tarhzoute
AZROU
Michlifène
TRETTENE
Bou Ibalrhatène
Lechmine n-Tajine
ATLAS
AIT HAMZA
MIDDLE
NORTH
TIZI
AIN LEUH
Bou-Tagarouine
TIMAHDITE
M.F.
AIN KAHLA
MRIRT
RP 24
Si Mguid
Tabourite
El Hammam
Foum Kheneg
Tsezmont
BEKRITE
RP 20
Oulmalne
Aguelmane Sidi Ali
Amengous
TAOUERDA
Lougnia
TAMAYOUST
AIT OUFELLA
ITZER
BOUMIA
Tounguejid
RP 21
MIDELT
Scale
0
10
20 km
10°
5°
Tanger
Alboran sea
Negene and quaternary volcanism
RIF
35°
Oujda
Rabat
Fès
Atlantic ocean
MIDDLE ATLAS
HIGH
ATLAS
Sirous
ANTI - ATLAS
Agadir
30°
0
100
200 km
Legend
Basement and cover sedimentary rocks
Eocene to Quaternary sedimentary rocks
Cretaceous sedimentary rocks
Jurassic sedimentary rocks
Triassic sedimentary rocks & CAMP basalts
Paleozoïc basement
Neogene and Quaternary volcanism
Strombolian cones, Maars
Subalkalic basalts
Alkali basalts
Basanites
Nephelinites
Roads and tracks
Cities and towns
Faults

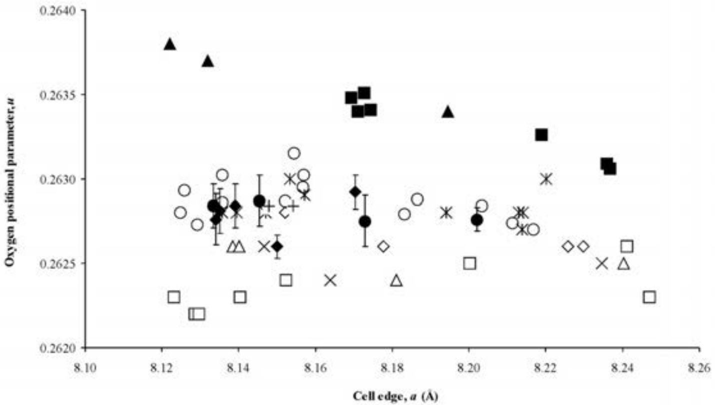
0.2640
0.2635
0.2630
0.2625
0.2620
8.10
8.12
8.14
8.16
8.18
8.20
8.22
8.24
8.26
Oxygen positional parameter, u
Cell edge, a (Å)

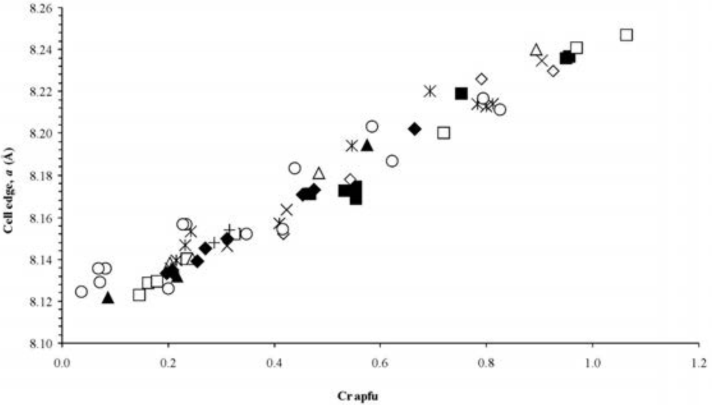

8.26
8.24
8.22
8.20
8.18
8.16
8.14
8.12
8.10
Cell edge, a (Å)
0.0
0.2
0.4
0.6
0.8
1.0
1.2
Cr apfu

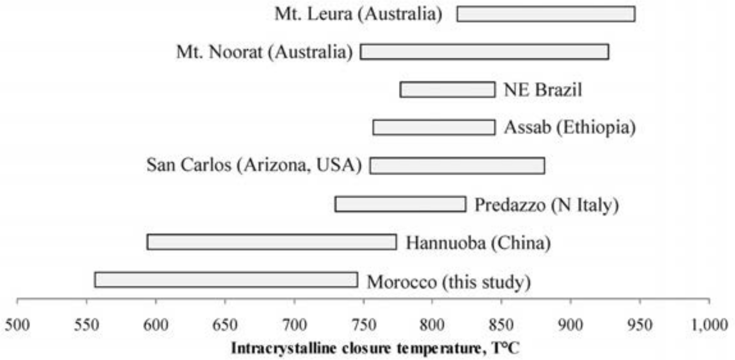

Mt. Leura (Australia)
Mt. Noorat (Australia)
NE Brazil
Assab (Ethiopia)
San Carlos (Arizona, USA)
Predazzo (N Italy)
Hannuoba (China)
Morocco (this study)
500
550
600
650
700
750
800
850
900
950
1,000
Intracrystalline closure temperature, T°C

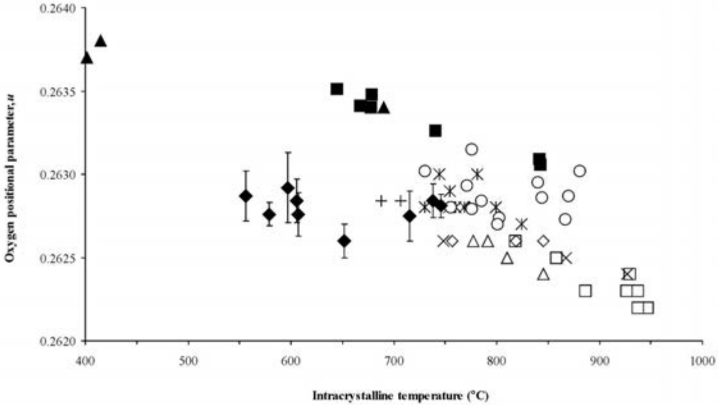
0.2640
0.2635
0.2630
0.2625
0.2620
Oxygen positional parameter, u
400
500
600
700
800
900
1000
Intracrystalline temperature (°C)

Sample	**MAR-BI2**	**MAR-BI4**	**MAR-BI16**	**MAR-BI24**	**MAR-TF6**	**MAR-TF7**	**MAR-TF8**	**MAR-TF21**	**MAR-TF28**
a	8.1334 (4)	8.1454 (5)	8.2021 (2)	8.1727 (5)	8.1339 (3)	8.13506 (9)	8.1704 (4)	8.1391 (6)	8.1499 (2)
u	0.2628 (1)	0.2628 (1)	0.26275 (7)	0.2627 (2)	0.2628 (1)	0.26283 (7)	0.2629 (2)	0.26285 (9)	0.2626 (1)
T-O	1.942 (2)	1.946 (2)	1.957 (1)	1.950 (2)	1.941 (2)	1.942 (1)	1.952 (3)	1.943 (1)	1.942 (1)
M-O	1.935 (1)	1.938 (1)	1.9516 (5)	1.945 (1)	1.935 (1)	1.9351 (5)	1.943 (2)	1.9358 (7)	1.9402 (7)
m.a.n.T	15.4 (2)	15.2 (5)	17.4 (1)	16.5 (4)	15.4 (2)	15.3 (2)	16.2 (4)	15.8 (3)	15.3 (2)
m.a.n.M	14.3 (2)	15.6 (4)	16.0 (2)	16.3 (3)	14.6 (2)	14.32 (9)	16.2 (5)	15.2 (3)	15.1 (3)
U (M)	0.0043 (3)	0.0057 (4)	0.0033 (1)	0.0054 (3)	0.0050 (3)	0.0041	0.0048 (4)	0.0053 (2)	0.0054 (2)
U (T)	0.0063 (4)	0.0070 (4)	0.0046 (2)	0.0079 (4)	0.0061 (3)	0.0060 (3)	0.0070 (5)	0.0069 (3)	0.0066 (3)
U (O)	0.0083 (4)	0.0081(5)	0.0062 (2)	0.0078 (5)	0.0081 (4)	0.0074 (2)	0.0074 (8)	0.0076 (3)	0.0085 (3)
N. refl.	114	125	169	112	113	157	100	133	133
R1	3.35	3.73	2.46	3.09	3.47	2.99	3.90	2.76	2.63
wR2	5.72	7.09	5.05	5.45	4.57	5.67	6.61	5.03	4.77
GooF	1.236	1.191	1.349	1.250	1.399	1.360	1.271	1.295	1.317
Diff.peaks	0.54; -1.30	1.03; -1.54	1.17; -1.29	0.69; -1.06	1.06; -0.72	0.74; -1.93	0.81; -1.00	0.55; -1.03	1.43; -0.65

Table 2: Results of structure refinement a_0: cell parameter (Å); *u*: oxygen positional parameter; T-O and M-O: tetrahedral and octahedral bond lenghts (Å), respectively; m.a.n.T and M: mean atomic number; U(M), U(T), U(O): displacement parameters for M site, T site and O; N. Refl.: number of unique reflections; R1 all (%), wR2 (%), GooF as defined in Sheldrick (2008). Diff.peaks: maximum and minimum residual electron density ($\pm e/Å^3$). Space Group: Fd-3m. Origin fixed at –3m. Z=8. Reciprocal space range: $-19 \leq h \leq 19$; $0 \leq k \leq 19$; $0 \leq l \leq 19$. Estimated standard deviations in *brackets*.

Sample	MAR-BI2	MAR-BI4	MAR-BI16	MAR-BI24	MAR-TF6	MAR-TF7	MAR-TF8	MAR-TF21	MAR-TF28
MgO	21.0 (2)	20.4 (3)	17.4 (1)	19.0 (3)	20.6 (3)	21.0 (2)	18.9 (3)	20.6 (3)	20.1 (3)
Al_2O_3	55.7 (4)	52.6 (4)	36.0 (2)	44.1 (4)	55.9 (5)	55.5 (4)	44.8 (3)	53.8 (3)	51.1 (3)
TiO_2	0.12 (2)	0.10 (2)	0.20 (2)	0.10 (1)	0.10 (2)	0.16 (2)	0.19 (2)	0.18 83)	0.15 (1)
Cr_2O_3	9.58 (9)	13.0 (2)	29.6 (3)	21.69 (2)	10.1 (1)	10.1 (1)	21.1 (2)	12.3 (1)	14.8 (2)
MnO	0.11 (3)	0.11 (3)	0.15 (3)	0.13 (2)	0.11 (3)	0.08 (2)	0.13 (3)	0.09 (3)	0.11 (3)
FeO_{tot}	12.1 (2)	12.9 (1)	16.2 (1)	13.8 (1)	12.1 (1)	11.9 (1)	14.0 (2)	12.1 (2)	12.6 (2)
NiO	0.40 (3)	0.37 (3)	0.27 (2)	0.28 (3)	0.41 (2)	0.40 (3)	0.33 (5)	0.37 (3)	0.34 (4)
ZnO	0.09 (3)	0.11 (4)	0.10 (4)	0.09 (3)	0.10 (4)	0.10 (4)	0.11 (3)	0.09 (4)	0.13 (5)
Sum	99.13	99.55	99.93	99.37	99.43	99.23	99.51	99.51	99.27
FeO	8.0 (2)	8.6 (1)	10.9 (1)	9.4 (1)	8.7 (1)	8.1 (1)	9.8 (2)	8.6 (2)	8.8 (2)
Fe_2O_3	4.5	4.8	5.9	4.8	3.8	4.3	4.7	3.9	4.3
Sum	99.58	100.03	100.51	99.85	99.81	99.66	99.98	99.91	99.70
T site									
Mg	0.674 (6)	0.713 (8)	0.682 (5)	0.627 (9)	0.681 (8)	0.652 (6)	0.673 (8)	0.634 (7)	0.694 (8)
Al	0.100 (2)	0.079 (2)	0.032 (1)	0.082 (2)	0.100 (2)	0.137 (2)	0.060 (2)	0.124 (2)	0.098 (2)
Mn	0.002 (1)	0.003 (1)	0.004 (1)	0.003 (1)	0.002 (1)	0.002 (1)	0.003 (1)	0.002 (1)	0.003 (1)
Fe^{2+}	0.133 (3)	0.109 (2)	0.182 (3)	0.199 (3)	0.137 (3)	0.160 (3)	0.185 (3)	0.181 (3)	0.120 (4)
Fe^{3+}	0.089 (6)	0.095 (7)	0.098 (4)	0.086 (7)	0.077 (7)	0.049 (4)	0.076 (6)	0.057 (6)	0.083 (7)
Zn	0.002 (1)	0.002 (1)	0.002 (1)	0.002 (1)	0.002 (1)	0.002 (1)	0.002 (1)	0.002 (1)	0.003 (1)
M site									
Mg	0.139 (3)	0.086 (3)	0.048 (1)	0.147 (4)	0.117 (3)	0.161 (3)	0.093 (3)	0.169 (4)	0.101 (3)
Al	1.611 (7)	1.554 (8)	1.173 (6)	1.340 (9)	1.613 (9)	1.569 (7)	1.384 (8)	1.537 (8)	1.502 (8)
Ti	0.002 (1)	0.002 (1)	0.004 (1)	0.002 1)	0.002 (1)	0.003 (1)	0.004 (1)	0.003 (1)	0.003 (1)
Cr	0.197 (2)	0.270 (5)	0.664 (6)	0.474 (5)	0.208 (3)	0.207 (3)	0.454 (4)	0.255 (3)	0.311 (4)
Fe^{2+}	0.042 (2)	0.080 (2)	0.076 (2)	0.017 (1)	0.052 (2)	0.017 (1)	0.038 (1)	0.007 (1)	0.074 (3)
Fe^{3+}			0.027 (2)	0.013 (3)		0.034 (4)	0.019 (3)	0.021 (3)	0.002 (1)
Ni	0.009 (1)	0.008 (1)	0.006 (1)	0.006 (1)	0.009 (1)	0.009 (1)	0.008 (1)	0.008 (1)	0.007 (1)
F(X)	0.11	0.25	0.17	0.25	0.44	0.42	0.19	0.49	0.23
T°C	605	556	579	716	607	746	597	738	652

Table 3 Chemical analyses and cation distribution. Mean chemical analyses (up to 15 spot analyses for each crystal) and cation distribution in T and M site of the analyzed Cr-spinels on the basis of four oxygen atoms per formula unit. Fe^{3+} from stoichiometry. F(x): minimization factor which takes into account the mean of square differences between calculated and observed parameters, divided by their standard deviations. Estimated standard deviations are in brackets. Intracrystalline closure temperature calculated by using the thermometer by Princivalle et al (1999).